

Flow field-induced drag forces and swimming behavior of three benthic fish species

Joschka Wiegleb^a, Philipp E. Hirsch^a, Bernd Egger^a, Frank Seidel^b, Patricia Burkhardt-Holm^{a,*}

^a Program Man-Society-Environment, Department of Environmental Sciences, University of Basel, Vesalgasse 1, 4051, Basel, Switzerland

^b Institute for Water and River Basin Management, Karlsruher Institute for Technology, Kaiserstrasse 12, 76131, Karlsruhe, Germany

ARTICLE INFO

Keywords:

Drag force
Benthic fish
Bullhead
Gudgeon
Round goby
Flow resistance
Swimming

ABSTRACT

Modern ethohydraulics is the study of the behavioral responses of swimming fish to flow fields. However, the exact drag forces experienced by fish remain poorly studied; this information is required to obtain a better understanding of the behavioral responses of fish and their current resistance strategies. We measured near-ground frontal drag forces on preserved individuals of three benthic fish species, round goby (*Neogobius melanostomus*), gudgeon (*Gobio gobio*) and bullhead (*Cottus gobio*), in a flow channel. The forces were compared to acoustic Doppler velocity (ADV) measurements and fish tracking data based on video observations of live fish in the flow channel. Overall, we observed drag coefficients (C_D) of $\sim 10^{-3}$ at Reynolds numbers $\sim 10^5$. The frontal drag forces acting on preserved fish with non-spread fins ranged from $-1.96 \text{ mN}\cdot\text{g}^{-1}$ (force per fish wet weight, velocity $0.55 \text{ m}\cdot\text{s}^{-1}$) to $11.01 \text{ mN}\cdot\text{g}^{-1}$ (velocity $0.85 \text{ m}\cdot\text{s}^{-1}$). Spreading the fins strongly increased the drag forces for bullhead and round goby. In contrast, the drag forces were similar for gudgeon with spread fins and all fish with non-spread fins. Video tracking revealed no clear relationship between the position of the fish in the flow field and the forces experienced by the preserved fish at these positions. Collectively, these results suggest that i) the differences in frontal drag forces between species are small in homogenous flow, ii) individuals chose their position in the flow field based on factors other than the drag forces experienced, and iii) whether fins are spread or non-spread is an essential quality that modulates species-specific differences. The methodology and results of this study will enable integration of flow measurements, fish behavior and force measurements and inform ethohydraulics research. More advanced force measurements will lead to a detailed understanding of the current resistance strategies of benthic fish and improve the design of fish passes.

1. Introduction

The successful passage of river barriers via fish passes is a global conservation goal and research topic (Katopodis and Williams, 2012; Williams et al., 2012). Successful passage depends on the physical and sensory capabilities, body morphology, behavior and movement phenology of the fish species (Rahel and McLaughlin, 2018). Flow measurements, fish behavior observations and modelling techniques are the main methods used to evaluate fish pass configurations (Wang et al., 2010; Puertas et al., 2012; Tsikata et al., 2014; Baki et al., 2016, 2017a, 2017b; Lima and Janzen, 2018). However, knowledge on the hydraulic preferences and swimming abilities of specific target species and life stages may enable the construction of fish passes with improved effectiveness, even for little-known benthic species (Williams et al., 2012). Laborde et al. (2020) pronounced the importance of further research on the characteristics of relevant species to enhance the

development of sustainable hydropower.

The literature indicates that specific, underappreciated hydrodynamic processes underlie benthic fish swimming. Most studies have focused on the performance of economically relevant fish in fish passes (Jansen et al., 1999; Aarestrup et al., 2003; Hirsch et al., 2016b). The swimming modes of benthic fish are less continuous than those of pelagic fish and rely more on intermediate or permanent contact with the ground. Body shape and pectoral fin usage are suggested to be highly relevant to the current resistance of benthic fish. Carlson and Lauder (2010) described the strategies used by benthic fish to resist currents with specialized body postures leading to negative lift forces. Flow field observations based on digital particle imaging close to the pectoral fins of Mottled sculpin (*Cottus bairdi*) revealed that the pectoral fins significantly altered the downstream flow field. These effects of the pectoral fins were suggested to increase negative lift forces and thereby increase station holding capability (Coombs et al., 2007).

* Corresponding author.

E-mail address: patricia.holm@unibas.ch (P. Burkhardt-Holm).

<https://doi.org/10.1016/j.limno.2020.125812>

Received 21 February 2020; Received in revised form 15 June 2020; Accepted 17 June 2020

Available online 18 August 2020

0075-9511/ © 2020 The Authors. Published by Elsevier GmbH. This is an open access article under the CC BY license (<http://creativecommons.org/licenses/by/4.0/>).

Even from a basic hydrophysical perspective, the drag forces acting on different benthic fish bodies are widely underappreciated. The kinematics of station holding by darter fish were estimated based on behavioral and flow observations; subtle body shape differences between the tested species were assumed to lead to important differences in station holding ability (Drucker, 2003; Carlson and Lauder, 2010, 2011).

Hydrodynamic forces are increasingly being measured by engineers, with a focus on the construction of artificial devices that imitate swimming fish (Newman, 1973; Barrett et al., 1999; McLetchie, 2003). This progress in the field of hydraulics has not been matched by the biological perspective of ethohydraulics, as existing measurements do not account for the species-specific and individual morphological characteristics of the fish. Here, we aimed to advance the field of ethohydraulics by studying benthic fish swimming from both a biological perspective (body shape, fin position and movement behavior) and hydraulic perspective (flow field and drag forces).

The invasive round goby (*Neogobius melanostomus* Pallas, 1814) is amongst Europe's 100 worst invasive species (Hirsch et al., 2016a) and has also invaded numerous North American habitats (Brown and Stepien, 2009). This small benthic fish species is currently spreading upstream into ecologically valuable tributaries in several river systems across the globe (Kornis et al., 2012). The round goby is confronted by several fish passes during its invasive passages, which raises the question of how the round goby—a benthic fish species—is hydraulically challenged during its passage of fish passes compared to native benthic fish.

In this context, invasion of the round goby serves as an ideal model to determine the importance of the species-specific morphological characteristics used to overcome drag forces in fish passes. To approach this topic, we performed experiments with round goby and two native bottom-dwelling fish species that inhabit similar riverine habitats: the gudgeon (*Gobio gobio* L.) and bullhead (*Cottus gobio* L.). The rationale behind this three-species approach was to detect differences in the drag forces acting on various morphologies in the overall understudied category of benthic fish. The mechanisms behind these individual responses to flow depending on body shape and swimming behavior remain unclear. We aimed to fill this knowledge gap with a three-pronged experimental approach in a swim canal by: 1. quantifying flow velocity in the flow field; 2. measuring the frontal drag forces acting on preserved fish bodies in a flow field; and 3. tracking the positions of live individuals in the flow field. Based on our video observations of living fish in currents, the preserved fish mimicked the body postures of live fish while swimming against flow. We expected homogenous flow conditions in the measuring chamber of the swim channel due to the flow straighteners in the flow channel (experiment 1). Furthermore, we expected body shape and fin variation to lead to differences in the frontal drag forces and their relationship with flow velocity. Thus, we measured the frontal drag forces for similarly sized preserved fish of all three species with spread and non-spread fins at one position in the swim channel while ramping up the flow velocity (experiment 2). Under the assumption that the swim channel creates a homogenous flow field but that the fish respond individually to local flow conditions based on their morphological characteristics, we expected to observe differences in the frontal drag forces depending on the specific location of different body shapes within the flow field. Therefore, we created maps of the drag forces experienced by the fish models at different locations in the flow field (experiment 3). Finally, under the assumption that fish behaviorally modulate the frontal drag forces they experience by changing their position within the swim canal, we expected that live individuals would spend more time at locations with lower frontal drag forces in the measuring chamber. Therefore, we video tracked the positions of live individuals across the chamber at different flow velocities (experiment 4).

2. Materials and methods

2.1. Fish sampling

Round goby ($n = 26$) were sampled between May and October 2018 in the River Rhine in Basel, Switzerland, using minnow traps baited with dog food. Native species were sampled in June 2018 in tributaries of the River Rhine: bullhead ($n = 13$) in the Maispracherbach and Wintersingerbach creeks in Magden and gudgeon ($n = 23$) in the Spittelmattbach creek in Basel. All gudgeon, bullhead and 15 round goby were anaesthetized, marked with passive integrated transponders (PIT-Tags) and carefully transferred to aquaria in the University of Basel for swimming tests. All remaining round goby ($n = 11$) were euthanized immediately after catching by an overdose of MS-222 and transported to the lab for preservation. Total length (T_L) in cm and wet weight (W_W) in g (Mettler Toledo PL1502-S) were determined in the lab. The round goby were sexed based on sexual dimorphism (Kornis et al., 2012). We could not unambiguously identify the sex of gudgeon or bullhead.

2.2. Ethics statement

All experiments were conducted according to local and federal law under permission Number 2934 of the Veterinary Office Basel Stadt.

2.3. Fish preservation

Nine round goby ($T_L = 9.63 \text{ cm} \pm 1.91$ [standard deviation], $W_W = 12.95 \text{ g} \pm 10.15$), 11 gudgeon ($T_L = 11.04 \text{ cm} \pm 1.41$, $W_W = 11.83 \text{ g} \pm 5.82$) and six bullhead ($T_L = 11.00 \text{ cm} \pm 0.61$, $W_W = 13.46 \text{ g} \pm 4.82$) were preserved with their fins laid onto their body, to achieve the non-spread fin treatment (nf). For all fish, fixation commenced with a bath of 4% formalin that completely covered the whole fish. This was done to avoid the effect of rigor mortis on fish flexibility and to maintain as comparable conditions between the fish as possible. To enable a comparison of only the effect of body shape on the forces experienced in the flow between the fish species, the bodies of the nf-treatment were adjusted to be as straight and symmetric as possible using needles before formalin fixation (S1). We assumed this body posture would provide the best representation of a fish overcoming increased current: when the fins are close to the body to decrease the body surface area exposed to the flow, as observed in the swimming videos of living fish.

The second group of fish were used to explore the effect of the fins on the frontal drag forces. We created a naturally spread fin configuration (sf treatment) for 17 round goby ($T_L = 11.11 \text{ cm} \pm 1.81$, $W_W = 18.20 \text{ g} \pm 9.79$), 12 gudgeon ($T_L = 10.73 \text{ cm} \pm 1.16$, $W_W = 10.59 \text{ g} \pm 4.53$) and seven bullhead ($T_L = 11.36 \text{ cm} \pm 1.30$, $W_W = 15.29 \text{ g} \pm 5.68$; S1). Needles were used to puncture the muscle tissues associated with the fins to spread the fins in a natural manner with as little impact on the body shape as possible.

After three days in the formalin solution, the fish were transferred through a graded series of ethanol solutions with increasing concentrations (24 h in 40 % ethanol, 24 h in 60 % ethanol and further storage in 75 % ethanol) to reduce shape changes of the fish induced in case of rapid concentration increases.

2.4. Force measuring device

A Vernier Go Direct Force and Acceleration Sensor (GDX-100609) and Vernier Graphical Analysis v4.4.0-945 software were used to measure the near-ground frontal drag forces acting on the fish in a swim tunnel (Loligo Systems, Swim Tunnel Respirometer #SW10250; 185 L volume, 88 * 25 * 25 cm measuring chamber). The sensor was fixed over the water surface (Fig. 1) and connected to a 50 cm long (3 mm-diameter) brass stick connected to a scaffold. A swivel connection

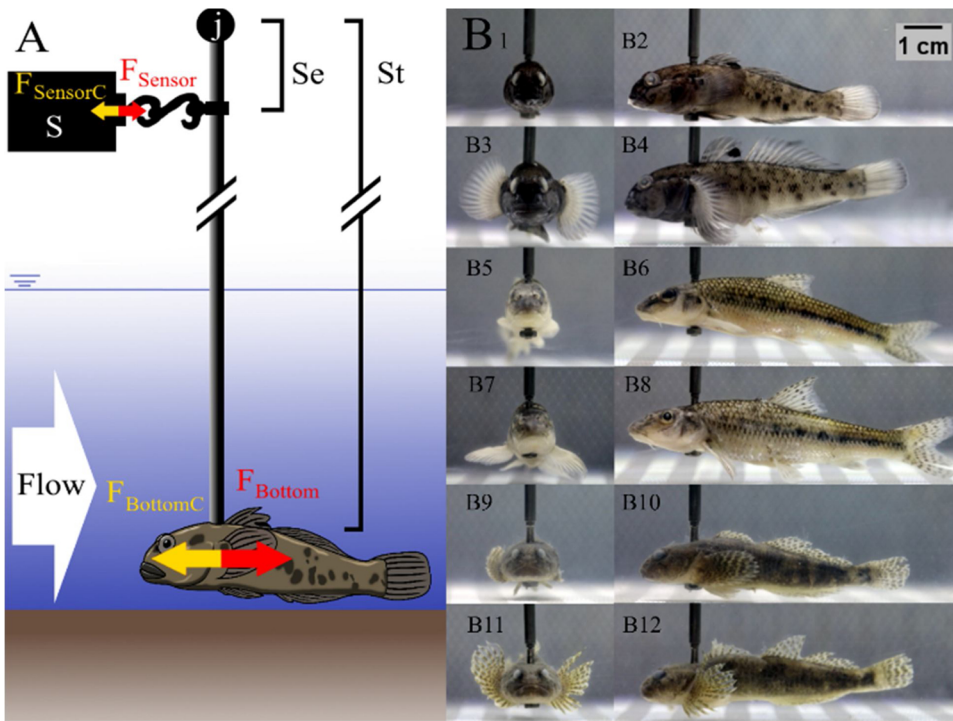


Fig. 1. Experimental setup (A) and the tested preserved individuals prior to the measurements in experiment 2 (B). The fish were fixed on the stick close to ground and the force (F_{Bottom}) induced by the flow was transduced to the sensor (S) via a joint (j) and a flexible clamp connection between the sensor and the stick. The distance between the fish and joint (St) and the distance between the sensor connection and joint (Se) were used to calculate the force acting on the fish (F_{Bottom}). The sensor was fixed on a scaffold, resulting in an opposing force ($F_{SensorC}$ and $F_{BottomC}$), keeping the fish in position. In experiment 2, the forces were measured for a single nf-round goby (B1, B2), sf-round goby (B3, B4), nf-gudgeon (B5, B6), sf-gudgeon (B7, B8), nf-bullhead (B9, B10) and sf-bullhead (B11, B12). The fish are displayed in frontal (odd numbers) and lateral (even numbers) views.

between the stick and scaffold ensured free oscillation of the stick on one axis. The sensor was connected to the stick 5 cm below the swivel via a flexible clamp connection. The drag force acting on the lower end of the stick with fish attached (F_{Bottom}) was calculated using the lever principle:

$$F_{Bottom} = F_{Sensor} * A$$

with F_{Sensor} representing the force detected by the sensor and A being the quotient between the entire fixation stick length ($St = 50$ cm) and the distance from the swivel to the sensor connection ($Se = 5$ cm; Fig. 1).

$$A = \frac{St}{Se} = \frac{50}{5} = 10$$

Reference measurements without fish were performed to account for the drag force of the flow field on the fixation stick. To determine the force acting only on the fish (F_{Fish}), the force acting on the stick (F_{Stick}) was subtracted from the forces measured when the fish were placed at the end of the stick (F_{Bottom}).

$$F_{Fish} = F_{Bottom} - F_{Stick}$$

Forty-five equidistant measurement points were chosen in the measuring chamber (Fig. 2, 4). The last row of measurement points in the downstream direction was located 10 cm upstream of the water outlet to ensure that the caudal fins of the preserved fish had no physical contact with the grid at the downstream end of the measuring chamber.

We exclusively measured frontal drag forces in the flow direction. The measuring device was adjusted to be exactly parallel to the flow channel plane, using spirit levels integrated into the scaffold. We maintained the distance to the ground (5–10 mm) and contact between the fish or stick and bottom was prevented to avoid the impact of uncontrolled friction on our measurements.

2.5. Force measurement procedure

The needles were removed from the preserved fish. After fixation on the measurement device (Fig. 1), the fish were photographed (Canon EOS 70D) in frontal and lateral view through the window in the

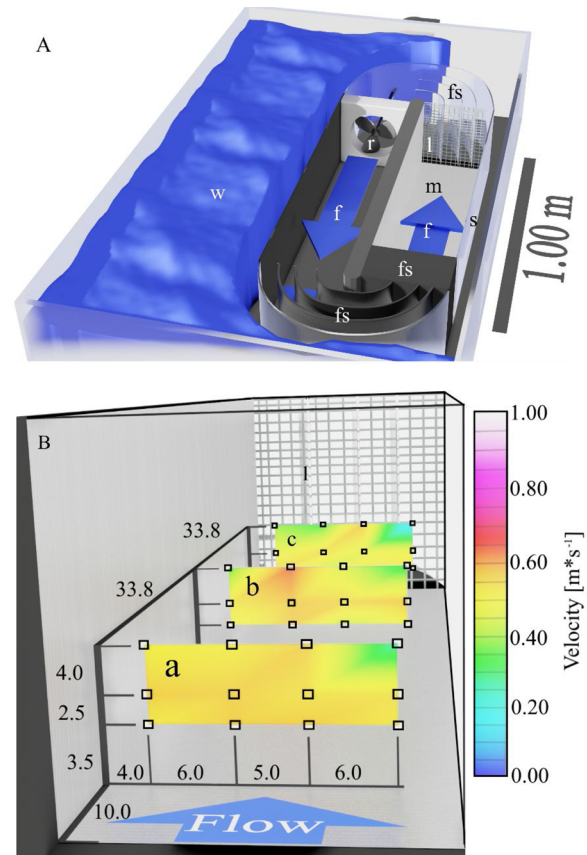


Fig. 2. Flow channel (A) with rotor (r), flow straighteners (fs), flow direction (f), window (s) and lattice (l). Fish were prevented from leaving the measurement chamber (m) by flow straighteners (upstream) and the lattice (downstream). The water (w) had a depth of 29 cm and covered the whole flow channel. The flow velocity is provided for the $0.55 \text{ m} \cdot \text{s}^{-1}$ velocity step (B) with the locations of the acoustic Doppler (black squares) shown in three profiles (a, b, c) and distances in cm.

measuring chamber to determine the frontal projected surface area (FPSA) using ImageJ 1.52p. Then, the fish were adjusted over one measuring point and the sensor was reset to commence recording (zero velocity). The flow velocity was increased in a stepwise manner following a ramping design (see below) and frontal drag forces were measured for 60 s at each flow velocity step. A compilation of published data on benthic fish swimming performance found a positive relationship between size and swimming performance (Hirsch et al., 2016b). Therefore, we divided the drag force by the wet weight of the fish ($\text{mN}\cdot\text{g}^{-1}$) to account for the size of individual fish.

The pectoral fins of nf-bullhead tended to spread during the preservation process (Fig. 1B9); thus, we artificially attached the pectoral fins by sewing three needle stitches using cotton sewing thread in this experiment. Preservation was satisfactory for round goby and gudgeon, thus artificial attachment of the fins was not necessary for these species.

2.6. Experiment 1: velocity

Flow measurements were conducted in the swimming chamber using a Nortek Vectrino Acoustic Doppler Velocimeter with the probe directed downwards in three transverse profiles within the measuring chamber; each transverse profile contained 12 measurement points (Fig. 2B, a, b, c). Each measurement was performed for 4 min at a data collection rate of 25 Hz. The data were processed using WinADV software and the mean flow velocities were illustrated using Tecplot 360 (Tecplot Inc.) for each point as linear interpolated values. Due to temporal restrictions, the measurements were performed for three ramping design velocities that were considered relevant to benthic fish swimming: 0.25, 0.55 and $0.85 \text{ m}\cdot\text{s}^{-1}$ (Tudorache et al., 2008; Tierney et al., 2011).

2.7. Experiment 2: change in frontal drag force with velocity

This experiment was performed to determine the change in drag forces for the three species as velocity increased and the effect of fin position on the drag forces experienced. The measuring device was located over the center measuring point. Three individual nf- and sf-round goby, -gudgeon and -bullhead were adjusted one fish at a time on the fixation device and the drag forces were measured for 60 s at a rate of 100 Hz (to account for short-term fluctuations in the forces due to vortices) at velocities of 0.30, 0.35, 0.45, 0.55, 0.65, 0.75, 0.8, 0.85, 0.95, 1.05, 1.15 and $1.25 \text{ m}\cdot\text{s}^{-1}$ (Nakayama, 1999):

$$C_D = \frac{2 \cdot F_{\text{fish}}}{\rho \cdot u^2 \cdot \text{FPSA}}$$

with ρ being the density of water at 20°C ($998.2 \text{ Kg}\cdot\text{m}^{-3}$; Nakayama, 1999) and u being the velocity [$\text{m}\cdot\text{s}^{-1}$]. Additionally, we computed the Reynolds number (Re; Reynolds, 1883):

$$Re = \frac{\rho \cdot u \cdot T_L}{\eta}$$

with η being the dynamic viscosity of water at 20°C ($10^{-3} \text{ Pa}\cdot\text{s}$; Nakayama, 1999; Table 1).

Personal observations and fast Fourier transformation (FFT) of the reference drag forces indicated a sudden and steep increase in vibration of the stick at velocities greater than $1.0 \text{ m}\cdot\text{s}^{-1}$ (S2). Therefore, we only included data recorded at velocities lower than $1.0 \text{ m}\cdot\text{s}^{-1}$ in our analysis.

2.8. Experiment 3: force maps

Single preserved nf-round goby, nf-gudgeon and nf-bullhead specimens were tested at different locations in the measuring chamber (Fig. 2) to compare the local forces experienced with the positions of live fish at the same velocities (experiment 4). The frontal drag forces

Table 1

Mean velocities and standard deviation (SD) determined by acoustic Doppler in the measurement chamber for the different profiles (Fig. 2).

| Channel Velocity [$\text{m}\cdot\text{s}^{-1}$] | Profile | Mean Velocity [$\text{m}\cdot\text{s}^{-1}$] | SD |
|---|---------|--|-------|
| 0.25 | a | 0.239 | 0.062 |
| | b | 0.257 | 0.059 |
| | c | 0.208 | 0.065 |
| 0.55 | a | 0.523 | 0.086 |
| | b | 0.496 | 0.097 |
| | c | 0.435 | 0.124 |
| 0.85 | a | 0.801 | 0.031 |
| | b | 0.796 | 0.081 |
| | c | 0.763 | 0.039 |

were measured twice per second (2 Hz) over 60 s, resulting in 121 values per measurement point, treatment and velocity. To focus on the forces acting at different locations and at different velocities in the flow chamber, the measurements were performed for 45 measurement points at velocities of 0.25, 0.55 and $0.85 \text{ m}\cdot\text{s}^{-1}$ for every treatment. Using the *filled.contour()* function of the *ggplot2* package in R i386 3.5.1, we created maps of the forces measured at different locations (Fig. 4). Furthermore, we compared the forcemaps of the different treatments by correlation analysis (Spearman) using the *ggpubr* package and *cor()* function of R.

2.9. Experiment 4: tracking

The locations of live fish in the measuring chamber were extracted from videos generated for another study on the comparative swimming behaviour and performance of benthic fish species (Egger et al., in preparation). A transparent cover was placed over the measuring chamber to prevent fish jumping out of the water. After the fish were acclimatised for 20 min at zero velocity, the flow velocity was successively ramped up to 0.15, 0.25, 0.35, 0.45 and $0.55 \text{ m}\cdot\text{s}^{-1}$. Each velocity step was maintained for 10 min and the fish were filmed from directly above the swim tunnel using a GoPro Hero 4[®] camera. All footage was analysed using Solomon Coder software (vers. beta 17.03.22). The position of individual fish in the measurement chamber for each completed velocity step was tracked using idTracker vers. 2.1 (Perez-Escudero and de Polavieja, 2011). If a fish became fatigued, the experiment was stopped for that individual and all completed velocity steps were included in the tracking analysis. This resulted in footage ranging between 45 and 172 min per individual (S3).

The R package *vec2dtransf* version 1.1 (Carrillo, 2012) was used to correct for the slightly different camera positions between trials. Round goby and bullhead swam close to or a few centimeters above the ground. However, a few individual gudgeon also moved higher up in the chamber water column; some swam up to 10 cm above the ground. Since the swimming occurred above the ground across all trials overall, we focused on the x- and y-coordinates in the plane field of the chamber for our analyses. Scatter plots were created based on the x- and y-coordinates of the fish position in every video frame and projected on the force maps (experiment 2) to enable a visual comparison (Fig. 4).

3. Results

3.1. Experiment 1: velocity

The velocity measurements showed the flow field was relatively uniform overall, but also indicated some differences in the transverse and longitudinal profiles of the flow field in the measurement chamber (Fig. 2, Table 1). There was a skewness in the velocity distribution of the different profiles. The maximum measured flow velocities of profile b shifted slightly to the left (downstream view) compared to the

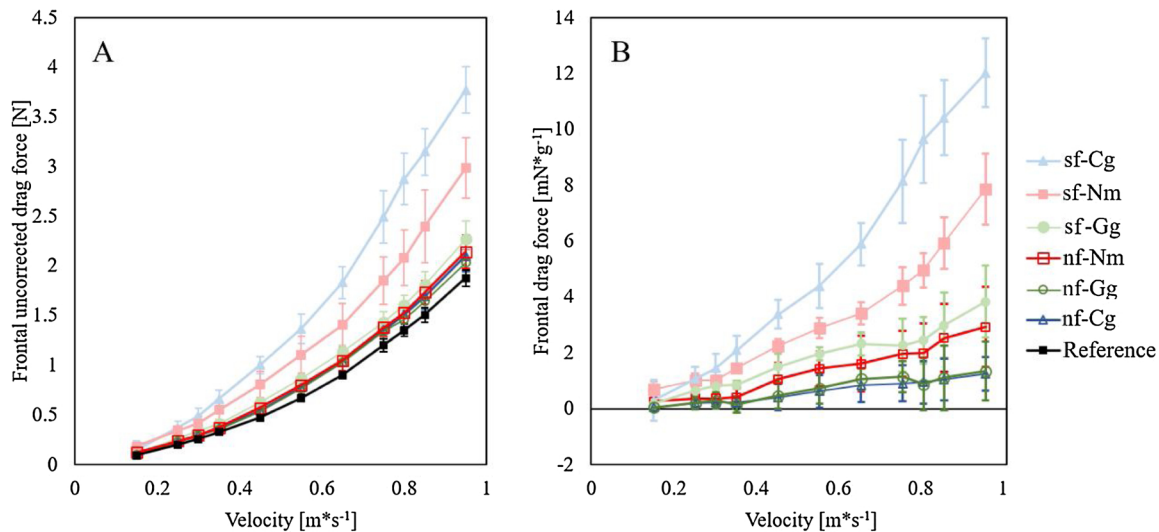


Fig. 3. Uncorrected forces acting on round goby (Nm), gudgeon (Gg) and bullhead (Cg) with spread fins (sf) and non-spread fins (nf) and the reference (fixation stick without fish) measured in the central location of the flow channel. Three individuals were tested for each group (A). The corrected forces (subtracted reference and division by the wet weight also increased with velocity (B).

upstream profile (Fig. 2a). This skewness together with the flow differences at the different profiles is assumed to result from the 180° arc of the flow induced by the shape of the flow channel (Fig. 2), which may have led to longitudinal velocity distribution variations.

3.2. Experiment 2: change in frontal drag force with velocity

The forces experienced by the preserved fish in the flow field increased with the velocity (Fig. 3). Larger frontal drag forces per fish weight were detected for sf-bullhead and sf-round goby, while the frontal drag forces acting on all nf-fish were rather small (maximum $2.93 \text{ mN}\cdot\text{g}^{-1} \pm 1.45 \text{ SD}$ for nf-round goby at $0.95 \text{ m}\cdot\text{s}^{-1}$). As flow velocity increased, the forces acting on sf-gudgeon were similar to all nf-fish. This, together with the percentage of FPSA induced by the pectoral fins being reduced for sf-gudgeon compared to sf-bullhead and sf-round goby (Table 2), suggests that the pectoral fins of gudgeon have the smallest impact on the frontal drag forces experienced of all tested species. The mean percentage of FPSA induced by the pectoral fins for sf-gudgeon was $23.63 \% \pm 2.39 \text{ SD}$, for sf-round goby $51.51 \% \pm 4.02 \text{ SD}$ and for sf-bullhead $48.96 \% \pm 3.8 \text{ SD}$. The proportion of FPSA induced by the fins for the nf-fish was generally smaller: $3.09 \% \pm 5.36 \text{ SD}$ for round goby, $2.90 \pm 5.02 \text{ SD}$ for gudgeon and $1.05 \pm 1.43 \text{ SD}$ for bullhead. In addition, the point of fin insertion is more ventrally located and extends over a smaller area than in the other species, which likely contributes to reduced forces in sf-gudgeon (Fig. 1B).

Considering the FPSA of the preserved fish (Table 2), the frontal drag forces of the different treatments were in accordance with the FPSA exposed to the current. At high FPSA, a large frontal drag force was observed; sf-bullhead had the largest recorded FPSA (Table 2) and largest frontal drag forces of all tested treatments (Fig. 3). In contrast, smaller frontal drag forces were detected at lower FPSA (e.g. nf-gudgeon).

The largest influence of fin position on FPSA was observed for bullhead, with a difference of 2.33 cm^2 of the mean FPSA between sf and nf, while the smallest impact was observed between sf- and nf-gudgeon (0.48 cm^2). The difference of the mean FPSA between sf- and nf-round goby was 1.97 cm^2 . This suggests that the spread fin-treatment increased the FPSA for bullhead and round goby and thus—unlike gudgeon—live bullhead and round goby can markedly affect the drag force they experience.

The C_D -values of sf-fish were highest for sf-bullhead ($8.19 \cdot 10^{-3}$) and lowest for sf-gudgeon ($4.10 \cdot 10^{-3}$), while the C_D -values of nf-fish

were highest for nf-round goby ($3.39 \cdot 10^{-3}$) and lowest for nf-bullhead ($1.81 \cdot 10^{-3}$) at a velocity of $0.95 \text{ m}\cdot\text{s}^{-1}$ and $Re \sim 1 \cdot 10^5$. In general, the sf-gudgeon displayed similar hydrodynamic characteristics to the nf-gudgeon. Up to 92.64 % of the drag force experienced by nf-gudgeon at $0.35 \text{ m}\cdot\text{s}^{-1}$ was induced by the fixation stick (reference). In contrast, the lowest proportion of drag force due to the reference was measured for sf-bullhead (47.00 % at $0.45 \text{ m}\cdot\text{s}^{-1}$). The forces measured on all nf-treatments were only slightly larger than the reference (Fig. 3), indicating the forces acting on nf-fish are generally small.

3.3. Experiment 3: force maps

Similarly to experiment 2, the drag forces experienced by the fish at the 45 different measurement points varied between the fin position treatments, fish species, and flow velocity. We recorded larger forces for sf-fish than nf-fish. The SDs of the frontal drag forces measured at different locations increased with velocity for every treatment (Table 3). Increasingly negative frontal drag forces were observed as velocity increased for nf-round goby. Positive frontal drag forces, which increased with velocity, were recorded for all sf-fish (Table 3).

The smallest mean frontal drag force, as well as the lowest FPSA, were observed for the nf-round goby compared to all other tested fish (Table 3). On the contrary, the sf-round goby displayed the largest FPSA of all treatments and experienced the largest frontal drag force. The smallest difference in FPSA between the two fin position treatments was observed for gudgeon (FPSA difference between sf- and nf-gudgeon was 21.03 % of the sf-gudgeon FPSA, for round goby 75.00 % and for bullhead 43.82 %). This was in agreement with small drag force differences between both fin position treatments (the difference became smaller as the velocity increased, up to the maximum difference of $4.75 \text{ mN}\cdot\text{g}^{-1}$ observed at a velocity of $1.15 \text{ m}\cdot\text{s}^{-1}$). This suggests fin position has minimal impact on the drag force experienced by gudgeon. Furthermore, the maximal frontal drag force observed for the nf-bullhead ($8.87 \text{ mN}\cdot\text{g}^{-1}$) was explicitly larger compared to the drag forces for nf-round goby ($-2.30 \text{ mN}\cdot\text{g}^{-1}$) and nf-gudgeon ($-0.87 \text{ mN}\cdot\text{g}^{-1}$); this may be related to the slightly spread pectoral fin of the preserved nf-bullhead (Fig. 1B9), suggesting that small variations in fin adjustment (such as slightly spread fins) can also have a large impact on the frontal drag forces experienced.

3.3.1. Force correlations

The spatial distribution of frontal drag forces was compared

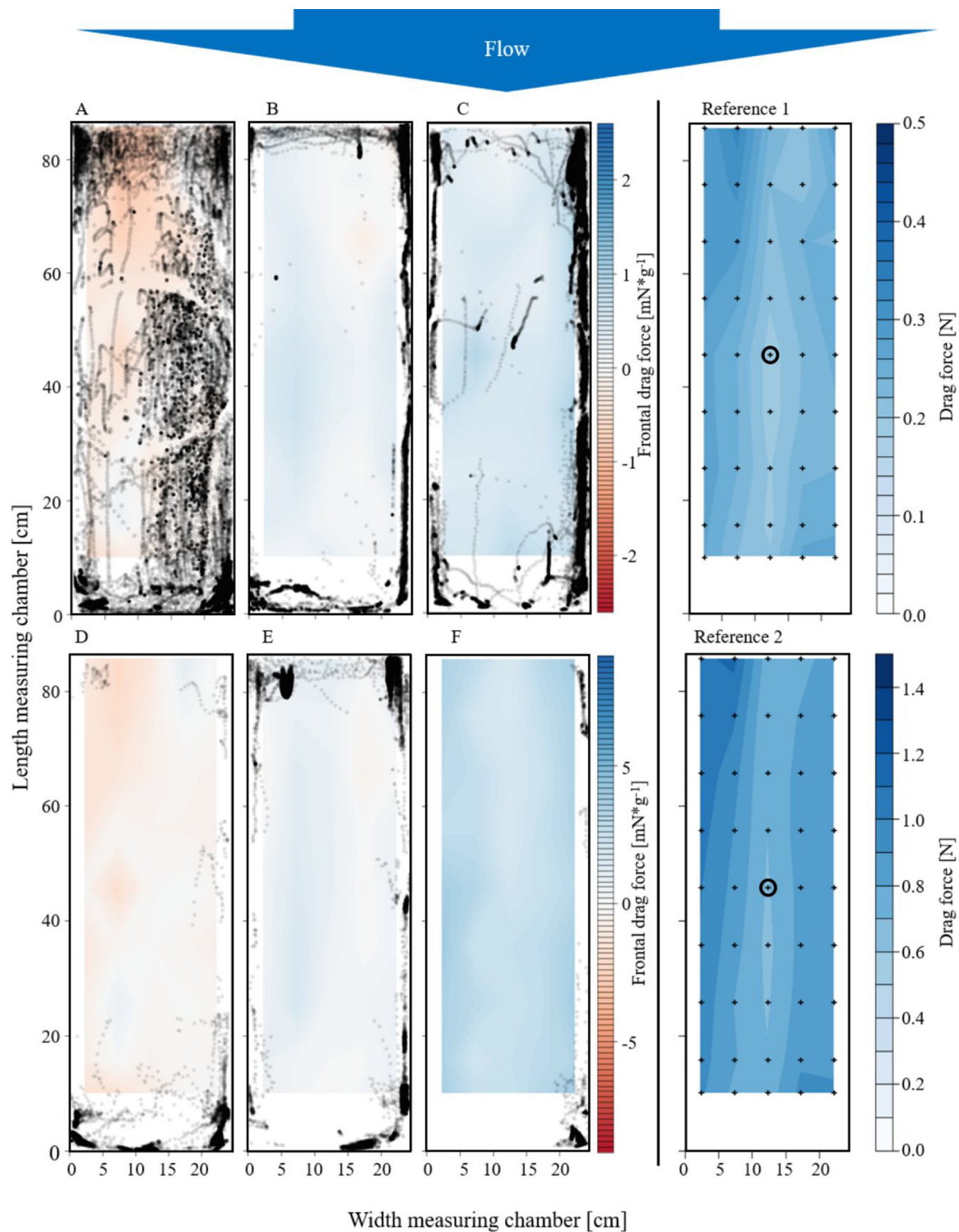


Fig. 4. Bird's-eye view of the measuring chamber at a velocity of $0.25 \text{ m} \cdot \text{s}^{-1}$ for nf-round goby (A), nf-gudgeon (B) and nf-bullhead (C) and at velocity of $0.55 \text{ m} \cdot \text{s}^{-1}$ for nf-round goby (D), nf-gudgeon (E) and nf-bullhead (F) showing the frontal drag forces at the related locations. Grey dots represent the presence of one fish in one video frame in the measuring chamber. The drag force acting on the fixation stick is displayed for velocities of $0.25 \text{ m} \cdot \text{s}^{-1}$ (Reference 1) and $0.55 \text{ m} \cdot \text{s}^{-1}$ (Reference 2). The measurement points ($n = 45$) are represented by black crosses at the references and the central point applied in experiment 1 is marked by black circles.

between round goby and the two other species by correlation analysis (Fig. 6). The 95 % confidence ellipses of sf-fish, separated from the ellipses of the nf-fish, were in agreement with the findings of experiment 2: the sf-fish experienced larger frontal drag forces than the nf-fish.

Furthermore, the nf- and sf-bullhead experienced stronger frontal drag forces than gudgeon at 0.55 and $0.85 \text{ m} \cdot \text{s}^{-1}$ (Fig. 6B, C). As

inferred from the point clouds around the dashed line, the frontal drag forces acting on sf-bullhead were similar to those experienced by sf-round goby at 0.25 , 0.55 and $0.85 \text{ m} \cdot \text{s}^{-1}$ (Fig. 6A, B, C). In contrast, the frontal forces acting on nf-bullhead were always larger than the forces on nf-round goby.

The frontal forces acting on sf-gudgeon were always smaller than the forces acting on sf-round goby. However, at velocities of 0.25 , 0.55

Table 2

Total length (T_L), wet weight (W_W), frontal projected surface area (FPSA), the proportion of the pectoral fins of the total FPSA (Fin FPSA), drag coefficients (C_D) and Reynolds numbers (Re) measured for round goby (Nm), gudgeon (Gg) and bullhead (Cg) with spread fins (sf) and non-spread fins (nf) in experiment 2 at a velocity of $0.95 \text{ m}\cdot\text{s}^{-1}$.

| Fish ID | T_L [cm] | W_W [g] | sex | FPSA [cm ²] | Fin FPSA [%] | Mean FPSA [cm ²] | \pm SD FPSA [cm ²] | C_D ($\cdot 10^{-3}$) | Mean C_D ($\cdot 10^{-3}$) | SD C_D ($\cdot 10^{-3}$) | Re ($\cdot 10^5$) | Mean Re ($\cdot 10^5$) | SD Re ($\cdot 10^5$) |
|---------|------------|-----------|--------------|-------------------------|--------------|------------------------------|----------------------------------|---------------------------|--------------------------------|------------------------------|---------------------|--------------------------|------------------------|
| sf-Nm-1 | 8.8 | 8.38 | female | 2.01 | 46.97 | 3.61 | 1.77 | 7.41 | 6.71 | 1.34 | 0.76 | 0.95 | 0.18 |
| sf-Nm-2 | 10.1 | 14.21 | male | 3.29 | 52.98 | | | 7.57 | | | 0.96 | | |
| sf-Nm-3 | 11.8 | 21.73 | male | 5.52 | 54.58 | | | 5.17 | | | 1.12 | | |
| sf-Gg-1 | 11.1 | 10.49 | undetermined | 1.55 | 22.13 | 2.12 | 0.65 | 6.14 | 4.10 | 2.34 | 1.05 | 1.05 | 0.03 |
| sf-Gg-2 | 11.3 | 10.49 | undetermined | 2.22 | 22.39 | | | 4.59 | | | 1.07 | | |
| sf-Gg-3 | 10.7 | 9.12 | undetermined | 2.85 | 26.39 | | | 1.55 | | | 1.01 | | |
| sf-Cg-1 | 10.8 | 15.68 | undetermined | 4.82 | 53.32 | 4.74 | 0.24 | 8.94 | 8.19 | 0.77 | 1.02 | 1.01 | 0.03 |
| sf-Cg-2 | 10.8 | 17.85 | undetermined | 4.93 | 47.26 | | | 8.22 | | | 1.02 | | |
| sf-Cg-3 | 10.3 | 13.87 | undetermined | 4.47 | 46.31 | | | 7.40 | | | 0.98 | | |
| nf-Nm-1 | 8.3 | 6.65 | female | 1.30 | 0.00 | 1.64 | 0.32 | 3.07 | 3.39 | 1.73 | 0.83 | 0.87 | 0.04 |
| nf-Nm-2 | 9.2 | 9.70 | female | 1.66 | 0.00 | | | 5.25 | | | 0.87 | | |
| nf-Nm-3 | 9.6 | 11.70 | female | 1.95 | 9.28 | | | 1.84 | | | 0.91 | | |
| nf-Gg-1 | 10.5 | 9.68 | undetermined | 1.53 | 8.69 | 1.69 | 0.40 | 3.31 | 1.90 | 1.31 | 1.00 | 1.06 | 0.14 |
| nf-Gg-2 | 12.9 | 18.49 | undetermined | 2.15 | 0.00 | | | 1.67 | | | 1.22 | | |
| nf-Gg-3 | 10.2 | 8.84 | undetermined | 1.40 | 0.00 | | | 0.73 | | | 0.97 | | |
| nf-Cg-1 | 10.8 | 15.49 | undetermined | 2.17 | 0.00 | 2.42 | 0.49 | 2.08 | 1.81 | 0.70 | 1.02 | 1.08 | 0.05 |
| nf-Cg-2 | 11.8 | 19.53 | undetermined | 2.98 | 2.68 | | | 2.35 | | | 1.12 | | |
| nf-Cg-3 | 11.5 | 17.93 | undetermined | 2.10 | 0.48 | | | 1.02 | | | 1.09 | | |

and $0.85 \text{ m}\cdot\text{s}^{-1}$ the frontal forces acting on nf-gudgeon were larger than those experienced by nf-round goby at the majority of measurement points, although the ellipses overlapped with the dashed line.

The formation of point clouds inside the ellipses shows a degree of similarity in the forces experienced by bullhead and gudgeon compared to round goby. The majority of correlations were not significant, indicating a large discrepancy between how drag forces act on different species at increasing velocities (nf-gudgeon and nf-round goby at $0.25 \text{ m}\cdot\text{s}^{-1}$ [Fig. 5A, $r = 0.114$, $p = 0.45$], nf-gudgeon and nf-round goby at $0.55 \text{ m}\cdot\text{s}^{-1}$ [Fig. 6B, $r = -0.08$, $p = 0.59$], both fin position treatments for bullhead and round goby at $0.55 \text{ m}\cdot\text{s}^{-1}$ [Fig. 6B, sf: $r = 0.09$, $p = 0.55$; nf: $r = -0.01$, $p = 0.94$], nf-gudgeon and nf-round goby [$r = 0.13$, $p = 0.38$], as well as sf-bullhead and sf-round goby at $0.85 \text{ m}\cdot\text{s}^{-1}$ [$r = 0.18$, $p = 0.24$]; Fig. 6C). In contrast, we detected significant correlations for the other eight comparisons, which suggests local differences in the frontal drag forces experienced between species. For example, there was a significant positive correlation, indicating increased similarity, between both bullhead fin position treatments and round goby at $0.25 \text{ m}\cdot\text{s}^{-1}$ velocity (nf: $r = 0.43$, $p = 0.004$; sf: $r = 0.49$, $p = 0.001$). A similar positive correlation was observed between sf-gudgeon and sf-round goby ($r = 0.64$, $p < 0.01$). At a velocity of $0.55 \text{ m}\cdot\text{s}^{-1}$, a significant correlation was only detected between sf-gudgeon and sf-round goby ($r = 0.62$, $p < 0.01$). At $0.85 \text{ m}\cdot\text{s}^{-1}$, a significant correlation occurred between sf-gudgeon and sf-round goby ($r = 0.48$, $p < 0.01$), with a significant negative correlation between nf-bullhead and nf-round goby ($r = -0.46$, $p < 0.01$); this correlation

indicates that frontal drag forces were larger for round goby at locations where the frontal drag forces acting on bullhead were smaller, and vice versa. These data based on preserved fish support the notion that fish can reduce the drag forces they experience by changing their position within a small flow field.

Overall, the points representing the frontal drag forces measured at the central position in experiment 2 (Fig. 4, black circles) tended to cluster toward the center of the point clouds. Additionally, the points for sf-fish were close together and the points for nf-fish were close together. This indicates that the forces experienced by the tested fish were more similar in the center of the measurement chamber than at other locations.

3.4. Experiment 4: tracking

Tracking of the positions of live fish within the chamber revealed a high density of records near the sidewalls and corners of the measuring chamber (Fig. 4, 5). As these locations were outside the area covered by the force and flow measurements, further quantification of the relationship between the positions of the fish and forces was unreasonable. However, some important insight can be extracted from the graphical combinations of the fish positions and forces (Fig. 4). Generally, we observed position records reduced as velocity increased, resulting from increased fish fatigue at stronger velocities (Fig. 4). The highest number of fish movements (as inferred from the scatter of recorded positions across the measuring chamber) was detected for round goby

Table 3

Frontal projected surface area (FPSA), the proportion of the pectoral fins of the total FPSA (Fin FPSA), total length (T_L) and wet weight (W_W) and mean and standard deviation (SD) of frontal drag forces in $\text{mN}\cdot\text{g}^{-1}$ (mean) determined in experiment 3 for round goby (Nm), gudgeon (Gg) and bullhead (Cg) with spread (sf) and non-spread fins (nf) at different velocities ($\text{m}\cdot\text{s}^{-1}$).

| Fish ID | FPSA [cm ²] | Fin FPSA [%] | T_L [cm] | W_W [g] | $0.25 \text{ m}\cdot\text{s}^{-1}$ | | $0.55 \text{ m}\cdot\text{s}^{-1}$ | | $0.85 \text{ m}\cdot\text{s}^{-1}$ | | $1.15 \text{ m}\cdot\text{s}^{-1}$ | |
|---------|-------------------------|--------------|------------|-----------|------------------------------------|------|------------------------------------|------|------------------------------------|------|------------------------------------|------|
| | | | | | Mean | SD | Mean | SD | Mean | SD | Mean | SD |
| sf-Nm-4 | 5.36 | 55.39 | 8.00 | 7.81 | 1.83 | 0.49 | 5.88 | 1.48 | 11.50 | 4.25 | 10.48 | 5.33 |
| nf-Nm-4 | 1.34 | 0.00 | 9.00 | 9.43 | -0.26 | 0.31 | -0.51 | 0.81 | -1.68 | 1.79 | -2.30 | 3.54 |
| sf-Gg-4 | 2.71 | 33.39 | 11.80 | 15.01 | 1.05 | 0.33 | 2.55 | 0.86 | 4.72 | 1.99 | 3.88 | 2.61 |
| nf-Gg-4 | 2.14 | 11.87 | 11.40 | 11.26 | 0.21 | 0.23 | 0.53 | 0.61 | 0.48 | 2.08 | -0.87 | 2.98 |
| sf-Cg-4 | 3.39 | 62.15 | 9.90 | 11.42 | 1.69 | 0.31 | 6.22 | 0.99 | 14.40 | 2.19 | 18.42 | 4.29 |
| nf-Cg-4 | 1.90 | 17.63 | 9.30 | 9.18 | 0.54 | 0.25 | 2.89 | 0.77 | 7.20 | 2.45 | 8.87 | 3.18 |

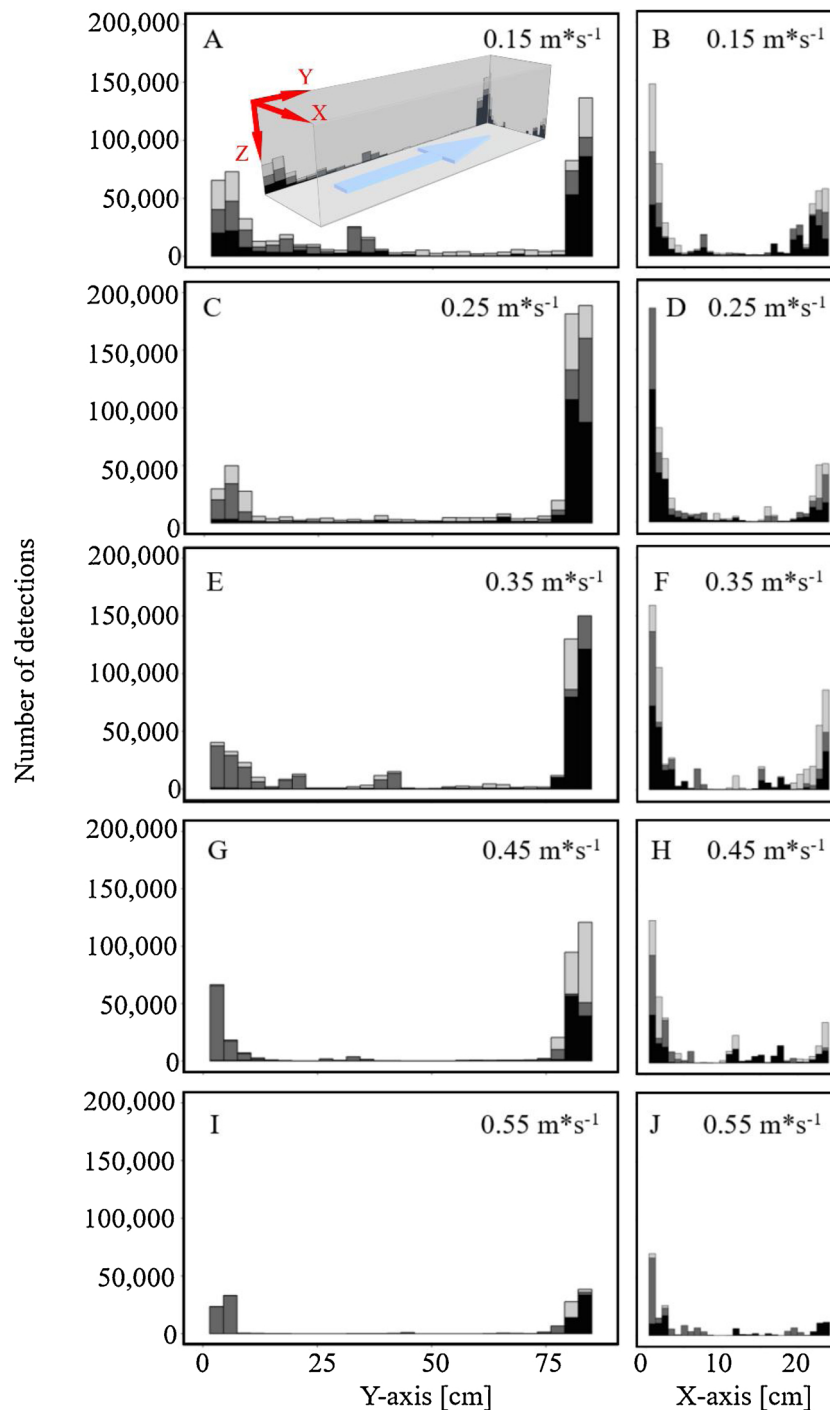


Fig. 5. Planar distribution of fish detections from the tracking analysis in the measurement chamber at different velocities ($\text{m}\cdot\text{s}^{-1}$) for round goby (black), gudgeon (grey) and bullhead (bright grey). View orientation is provided in a drawing of the measuring chamber (A) with the flow direction indicated (blue arrow). Each single recording across all the video frames for each individual and for each velocity step was recorded and stacked as a summed histogram, thus illustrating the individuals' whereabouts during the experiment.

at $0.25 \text{ m}\cdot\text{s}^{-1}$, which was also the treatment with the lowest measured forces at this velocity (Fig. 4A). In contrast, the lowest fish activity (i.e. the fewest fish position records) was detected for bullhead at $0.55 \text{ m}\cdot\text{s}^{-1}$, when the strongest forces were measured. Reduced scattering of the position of round goby was observed at $0.55 \text{ m}\cdot\text{s}^{-1}$, when our measuring device detected the strongest negative frontal drag forces.

4. Discussion

The aim of this study was to increase our knowledge of how benthic

fish experience currents by comparing experimental drag force and flow measurements with fish tracking data. The frontal drag forces acting on fish depend on their fin position and location in the measurement chamber. In comparison to the strong effect of fin position on the frontal drag forces experienced by round goby and bullhead, the kind of species had a rather small effect on the forces experienced at both fin position treatments. The fins induced the most important interspecies differences in drag forces, indicating that live fish have divergent abilities to interact and manipulate the flow field surrounding their body (Carlson and Lauder, 2011). However, for gudgeon, their fins may

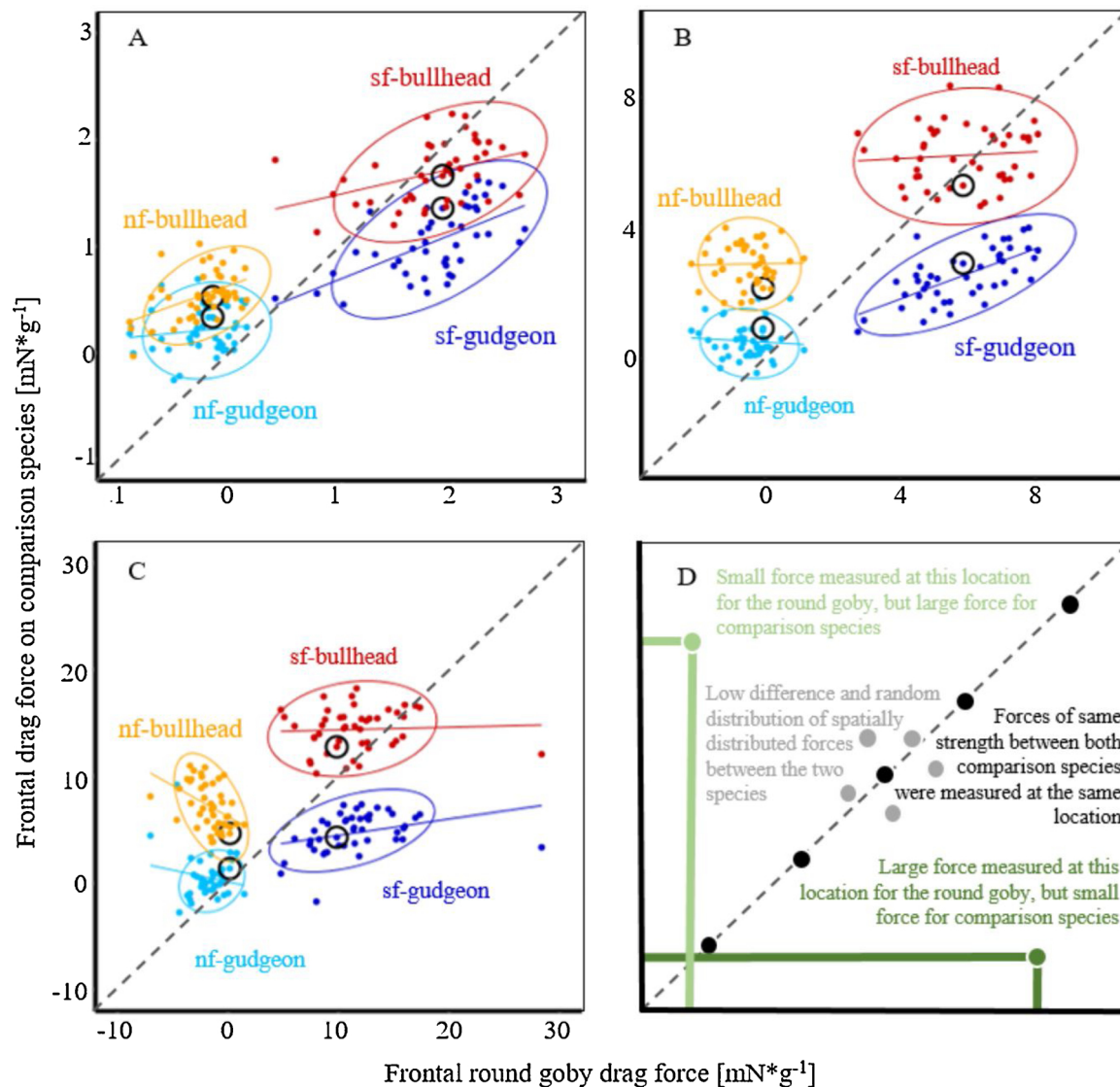


Fig. 6. Frontal drag force comparison by correlation between round goby and the two comparison species (bullhead and gudgeon) at velocities of 0.25 (A), 0.55 (B), and 0.85 $m*s^{-1}$ (C) for fish with spread fins (sf) and non-spread fins (nf) and reading instruction for this figure (D). Every point represents one measurement point in the flow chamber ($n = 45$). The measurement point of experiment 1 is marked by a black circle for every treatment.

have minimal impact on the frontal drag forces experienced. Due to the small impact of the pectoral fins on the frontal drag forces experienced by gudgeon and their strong swimming capabilities, it is possible that the pectoral fins of gudgeon mainly exert a piloting function. This swimming mode is in accordance with the BCF mode (body and/or caudal fin locomotion), characterized by propulsion through a wave moving backwards through the body and caudal fins (Sfakiotakis et al., 1999). This swimming mode and fin function may enable gudgeon to swim in the water column at higher velocities (as observed in experiment 3) and is in accordance with Tudorache et al. (2008), who reported unexpectedly high critical swimming speeds, even though gudgeon are assumed to be bottom-dwellers. When comparing the morphology, relative size, and insertion of the pectoral fins between gudgeon and round goby and bullhead, it appears that the gudgeon's pectoral fins might have a less important function in modulating negative lift forces (Coombs et al., 2007). In contrast, round goby and bullhead may use their pectoral fins and higher FPSA (compared to gudgeon) to produce negative lift forces to resist the current (personal observation; Koehl, 1984; Coombs et al., 2007; Tudorache et al., 2008; Carlson and Lauder, 2010). Although we did not measure lift forces, it is likely that both species are able to adjust their fins to vertically deflect

the frontal drag force to the ground and increase friction.

Round goby diverged from gudgeon and bullhead, especially in their ability to change FPSA. Furthermore, round goby experience much stronger negative frontal drag forces than gudgeon and bullhead. Together with previous work demonstrating the ability of round goby to switch between the BCF and MPF (median and/or paired fins) swimming modes (Pennuto and Rupprecht, 2016), we assume round goby may be able to adapt their swimming mode to local flow conditions. This behavior could enable round goby to overcome fish passes and aid their spread into upstream tributaries. This flexibility may be a compensation for the poor morphological specialization of round goby (Jakubčinová et al., 2017) and could be another factor that explains the invasive success of this species.

Initially, the negative frontal drag forces—especially for the nf-round goby in experiment 2—seemed counterintuitive. However, Beal et al. (2006) reported that the bodies of dead fish produce enough propulsion at specific vortex conditions to overcome their own drag and move against the direction of flow. As the flow was altered by the 180° arc of the flow channel (Fig. 2) and we detected the strongest negative drag forces in the upstream area of the flow channel, it is likely that such propulsion occurred in our experiment. This could create

beneficial hydrodynamic conditions for round goby, potentially reducing the muscle activity required while swimming, as described for trout (*Oncorhynchus mykiss*; Liao et al., 2003). This phenomenon was especially observed for nf-round goby, and can be formulated as the hypothesis that round goby have an advantage in currents over bullhead and gudgeon. However, the tracking data did not reveal more points at areas with negative forces, thus further tests are necessary to support this conclusion.

Apart from behavioral adaptation, morphological adaptations to currents have been described in fish (Imre et al., 2002; Franssen et al., 2013; Pennuto and Rupprecht, 2016). Body shape was observed to diverge between individuals from stream and reservoir habitats in a cyprinid species (Franssen et al., 2013) and Imre et al. (2002) found juvenile brook charr (*Salvelinus fontinalis*) that inhabited habitats with high flow velocities had larger caudal fins and more slender bodies compared to those from low velocity habitats. Due to our small sample size, we have to be careful when deriving conclusions related to body shape-induced differences. However, the variation in the locations of the point clouds and directions of the correlations varying with velocity for some fish in experiment 3 suggest that the frontal drag forces differ between species due to morphological differences. Together with our findings of the high impact of fin position and behavioral differences between species, it is likely that our approach of measuring the drag forces using preserved fish is promising to advance our knowledge of the interactions between hydrodynamics and benthic fish swimming. Most importantly, using preserved fish excludes the confounding factors affecting fish behavior (such as adaptation, condition and temperature).

Although the flow velocity varied within the measurement chamber, the live fish did not follow the patterns of reduced drag force and reduced velocities. Instead, the fish preferred locations close to the side walls. This is assumed to be a behavioral response of the fish to the flow, aiming at reducing energetic costs, as described by Cook and Coughlin (2010) for rainbow trout. Acoustic Doppler could not reliably quantify the flow directly above the surface and in the corners of the chamber, where the fish were frequently located. So, although we could not achieve a quantitative comparison of locations and forces, we can still relate the patterns observed to current scientific knowledge. Haro et al. (2004) reported the lowest velocities near the walls and floor of an open-channel flume. Based on general hydrodynamic observations, the flow characteristics in the corners of a rectangular channel strongly differ from the flow in the center of the channel. Mean velocity is reduced in the corners due to the shear effect and secondary flows developed (Chow, 1959). We assume that, in our study, boundary effects and the secondary flow field in the corners of the channel at locations close at the ground and close to the wall were more favorable to fish than the open area of the measurement chamber. The importance of behavioral effects is evident from the large number of locations recorded at the downstream water outlet grid, which indicates the majority of fish were not motivated to swim and rested near the grid, where the physical structure of the grid and vortices may have supported their body against the flow. However, these problems of individual motivation are avoided in force measurements of preserved fish, and allowed species-specific flow characterization of the flow fields acting on fish bodies without the need to test living individuals. Measurements of preserved fish provide a more accurate representation of the forces fish have to overcome when ascending a fish pass, as the results are independent of fish motivation and behavior. Measurement of frontal drag forces helps to understand the effort fish have to invest when overcoming currents, without using live experimental animals, which is beneficial in terms of the uncertainties of planning and conducting experiments with living animals. Although we can only measure one factor at a time, either force or behavior, the combinatory approach holds promise for quantification of forces, which we assume are relevant to behavior. In the context of invasive species such as the round goby, additional knowledge on forces and the behavioral

response of the fish on these forces may inform the design of fish passes in which currents are adapted to impede or facilitate the migration of specific target species (Williams et al., 2012).

As a result of our decision to use preserved fish, we focused on the physical response of the fish bodies based on the sum of morphological and body posture characteristics. This is a methodological novelty compared to previous studies that measured the forces acting on artificial fish models with over-simplified shapes (Newman, 1973; Barrett et al., 1999; McLetchie, 2003). The use of multidirectional force sensors in future experiments will greatly advance our ability to fully describe the forces experienced by the bodies of fish.

Hydraulic modelling and measurements of swim canals or large fishways have enabled substantial advancements in ethohydraulics in recent years (Plew et al., 2007; Lindberg et al., 2013). These measurements were interpreted in the context of direct visual (Plew et al., 2007) or indirect automated tracking information on fish behavior (Lindberg et al., 2013). To the best of our knowledge, fast-swimming ‘flagship’ species—which have rather large body sizes—have been the focus of ethology, rather than benthic fish (Plew et al., 2007; Lindberg et al., 2013). For example, Lindberg et al. (2013) elaborately modelled the flow below a hydropower tailrace in a Swedish river. These hydraulic data were combined with ethological data on the movements and positions of Atlantic Salmon (*Salmo salar* L.) below the tailrace. Combination of these datasets enabled identification of the optimal position for a planned fishway entrance. Using a similar approach, but under more controlled conditions, Plew et al. (2007) mapped a flow chamber using acoustic Doppler and then compared the variation in the swimming acceleration and maximum speed of a galaxiid (*Galaxius maculatus*) with the flow variations. Due to the typically low Reynolds number of fish bodies, major energy expenditure should be required to overcome the drag acting against the body, at least for carangiform or subcarangiform swimmers, the most common swimming types among temperate freshwater fish. Since the drag force is proportional to velocity squared, the fish should both minimize overall drag and also vary their swimming velocity to conserve energy (Anderson et al., 2001). Therefore, fish should follow the path with minimal drag forces that requires minimal acceleration. Our study is the first to quantify the drag forces acting on the bodies of fish. This data can now be used to advance existing procedures to study fish passage. However, we did not observe that benthic fish follow force patterns in homogenous flow, suggesting that other factors influence the swimming behavior of benthic fish beyond frontal drag forces alone. Our data has the potential to advance traditional approaches, such as hydraulic modelling of flow velocities in a fish-way. Gisen et al. (2017) used fish-size-speed relations based on an ethohydraulic scale to make conclusions related to fish migration corridors. Our data, in combination with living fish behavior tracked as movement corridors and vicinity to structures as two novel parameters, could advance these approaches. These novel parameters have the potential to generate more realistic fish swimming models.

CRedit authorship contribution statement

Joschka Wiegleb: Conceptualization, Investigation, Methodology, Software, Formal analysis, Writing - original draft, Visualization, Project administration, Validation. **Philipp E. Hirsch:** Conceptualization, Investigation, Methodology, Writing - original draft, Writing - review & editing. **Bernd Egger:** Conceptualization, Investigation, Methodology, Software, Formal analysis, Visualization, Writing - original draft, Writing - review & editing. **Frank Seidel:** Conceptualization, Investigation, Methodology, Software, Formal analysis, Visualization, Writing - original draft, Writing - review & editing. **Patricia Burkhardt-Holm:** Conceptualization, Investigation, Methodology, Writing - original draft, Writing - review & editing, Resources, Project administration.

Acknowledgements

This work was funded by the Federal Office for the Environment (FOEN; Contract-Nr. Q493-0660), Kantons Basel Stadt, as well as the Lotteriefunds of Basel Land, Aargau and Solothurn. We gratefully thank Peter Reimann, Laurent Marot and Marco Martina of the Department of Physics, University of Basel, and Georg Rauter, Department of Biomedical Engineering, University of Basel, for helpful advice and technical support. Furthermore, we thank Hans-Peter Jermann, cantonal fisheries officer Basel Stadt, for support with catching the fish, Johannes Hilpert, Karlsruhe Institute for Technology, for performing the flow measurements, Daniel Oosterwind, Thuenen Institute of Baltic Sea Fisheries, for critical review and helpful advice, the anonymous reviewers for their constructive advice, and Franziska Wiegleb for providing vital support.

Appendix A. Supplementary data

Supplementary material related to this article can be found, in the online version, at doi:<https://doi.org/10.1016/j.limno.2020.125812>.

References

- Aarestrup, K., Lucas, M.C., Hansen, J.A., 2003. Efficiency of a nature-like bypass channel for sea trout (*Salmo trutta*) ascending a small Danish stream studied by PIT telemetry. *Ecol. Freshw. Fish* 12 (3), 160–168. <https://doi.org/10.1034/j.1600-0633.2003.00028.x>.
- Anderson, E.J., McGillis, W.R., Grosenbaugh, M.A., 2001. The boundary layer of swimming fish. *J. Exp. Biol.* 204 (1), 81–102.
- Baki, A.B.M., Zhu, D.Z., Rajaratnam, N., 2016. Flow simulation in a rock-ramp fish pass. *J. Hydraul. Eng.* 142 (10), 04016031. [https://doi.org/10.1061/\(ASCE\)HY.1943-7900.0001166](https://doi.org/10.1061/(ASCE)HY.1943-7900.0001166).
- Baki, A.B.M., Zhu, D.Z., Harwood, A., Lewis, A., Healey, K., 2017a. Rock-weir fishway I: flow regimes and hydraulic characteristics. *J. Ecohydraulics* 2 (2), 122–141. <https://doi.org/10.1080/24705357.2017.1369182>.
- Baki, A.B.M., Zhu, D.Z., Harwood, A., Lewis, A., Healey, K., 2017b. Rock-weir fishway II: design evaluation and considerations. *J. Ecohydraulics* 2 (2), 142–152. <https://doi.org/10.1080/24705357.2017.1369183>.
- Barrett, D.S., Triantafyllou, M.S., Yue, D.K.P., Grosenbaugh, M.A., Wolfgang, M.J., 1999. Drag reduction in fish-like locomotion. *J. Fluid Mech.* 392, 183–212.
- Beal, D.N., Hover, F.S., Triantafyllou, M.S., Liao, J.C., Lauder, G.V., 2006. Passive propulsion in vortex wakes. *J. Fluid Mech.* 549, 385–402. <https://doi.org/10.1017/S0022112005007925>.
- Brown, E.J., Stepien, A.C., 2009. Invasion genetics of the Eurasian round goby in North America: tracing sources and spread patterns. *Mol. Ecol.* 18, 64–79. <https://doi.org/10.1111/j.1365-294X.2008.04014.x>.
- Carlson, R.L., Lauder, G.V., 2010. Living on the bottom: kinematics of benthic station-holding in darter fishes (percidae: Etheostominae). *J. Morphol.* 271 (1), 25–35. <https://doi.org/10.1002/jmor.10776>.
- Carlson, R.L., Lauder, G.V., 2011. Escaping the flow: boundary layer use by the darter *Etheostoma tetrazonum* (Percidae) during benthic station holding. *J. Exp. Biol.* 214 (7), 1181–1193. <https://doi.org/10.1242/jeb.051938>.
- Carrillo, G., 2012. Package ‘vec2dtrnsf’.
- Chow, V.T., 1959. *Open-Channel Hydraulics*. McGraw-Hill Book Company, London.
- Cook, C.L., Coughlin, D.J., 2010. Rainbow trout *Oncorhynchus mykiss* consume less energy when swimming near obstructions. *J. Fish Biol.* 77 (7), 1716–1723. <https://doi.org/10.1111/j.1095-8649.2010.02801.x>.
- Coombs, S., Anderson, E., Braun, C.B., Grosenbaugh, M., 2007. The hydrodynamic footprint of a benthic, sedentary fish in unidirectional flow. *J. Acoust. Soc. Am.* 122 (2), 1227–1237. <https://doi.org/10.1121/1.2749455>.
- Drucker, E.G., 2003. Function of pectoral fins in rainbow trout: behavioral repertoire and hydrodynamic forces. *J. Exp. Biol.* 206 (5), 813–826. <https://doi.org/10.1242/jeb.00139>.
- Franssen, N.R., Stewart, L.K., Schaefer, J.F., 2013. Morphological divergence and flow-induced phenotypic plasticity in a native fish from anthropogenically altered stream habitats. *Ecol. Evol.* 3 (14), 4648–4657. <https://doi.org/10.1002/ece3.842>.
- Gisen, D.C., Weichert, R.B., Nestler, J.M., 2017. Optimizing attraction flow for upstream fish passage at a hydropower dam employing 3D detached-eddy simulation. *Ecol. Eng.* 100, 344–353. <https://doi.org/10.1016/j.ecoleng.2016.10.065>.
- Haro, A., Castro-Santos, T., Noreika, J., Odeh, M., 2004. Swimming performance of upstream migrant fishes in open-channel flow: a new approach to predicting passage through velocity barriers. *Can. J. Fish. Aquat. Sci.* 1601 (1958), 1590–1601. <https://doi.org/10.1139/F04-093>.
- Hirsch, P.E., N’Guyen, A., Adrian-Kalchhauser, I., Burkhardt-Holm, P., 2016a. What do we really know about the impacts of one of the 100 worst invaders in Europe? A reality check. *AMBIO* 45 (3), 267–279. <https://doi.org/10.1007/s13280-015-0718-9>.
- Hirsch, P.E., Thorlacius, M., Brodin, T., Burkhardt-Holm, P., 2016b. An approach to incorporate individual personality in modeling fish dispersal across in-stream barriers. *Ecol. Evol.* 7 (2), 720–732. <https://doi.org/10.1002/ece3.2629>.
- Imre, I., McLaughlin, R.L., Noakes, D.L.G., 2002. Phenotypic plasticity in brook charr: changes in caudal fin. *J. Fish Biol.* 61 (5), 1171–1181. <https://doi.org/10.1006/jfbi.2002.2131>.
- Jakubčinová, K., Simonović, P., Števo, B., Čanak Atlagić, J., Kováč, V., 2017. What can morphology tell us about ecology of four invasive goby species? *J. Fish Biol.* 90 (5), 1999–2019. <https://doi.org/10.1111/jfb.13283>.
- Jansen, W., Kappus, B., Bohmer, J., Beiter, T., 1999. Fish communities and migrations in the vicinity of fishways in a regulated river (Enz, Baden-Württemberg, Germany). *Limnologia* 29 (4), 425–435.
- Katopodis, C., Williams, J.G., 2012. The development of fish passage research in a historical context. *Ecol. Eng.* 48, 8–18. <https://doi.org/10.1016/j.ecoleng.2011.07.004>.
- Koehl, M.A.R., 1984. How do benthic organisms withstand moving water? *Am. Zool.* 24 (1), 57–70.
- Kornis, M.S., Mercado-Silva, N., vander Zanden, M.J., 2012. Twenty years of invasion: a review of round goby *Neogobius melanostomus* biology, spread and ecological implications. *J. Fish Biol.* 80 (2), 235–285. <https://doi.org/10.1111/j.1095-8649.2011.03157.x>.
- Laborde, A., Habit, E., Link, O., Kemp, P., 2020. Strategic methodology to set priorities for sustainable hydropower development in a biodiversity hotspot. *Sci. Total Environ.* 714, 136735. <https://doi.org/10.1016/j.scitotenv.2020.136735>.
- Liao, J.C., Beal, D.N., Lauder, G.V., Triantafyllou, M.S., 2003. Fish exploiting vortices decrease muscle activity. *Science* 302, 1566–1569. <https://doi.org/10.1126/science.1088295>.
- Lindberg, D.E., Leonardsson, K., Andersson, A.G., Lundström, T.S., Lundqvist, H., 2013. Methods for locating the proper position of a planned fishway entrance near a hydropower tailrace. *Limnologia* 43 (5), 339–347. <https://doi.org/10.1016/j.limno.2013.05.007>.
- McLetchie, K.M.W., 2003. In: IEEE Cat. No. 03CH37492. Drag Reduction of an Elastic Fish Model. *Oceans 2003. Celebrating the Past... Teaming Toward the Future Vol. 5*. pp. SP2938–SP2944. <https://doi.org/10.1109/OCEANS.2003.178373>.
- Nakayama, Y., 1999. *Introduction to Fluid Mechanics*. Butterworth-Heinemann.
- Newman, J.N., 1973. The force on a slender fish-like body. *J. Fluid Mech.* 58 (4), 689–702. <https://doi.org/10.1017/S0022112073002429>.
- Pennuto, C.M., Ruppel, S.M., 2016. Upstream range expansion by invasive round gobies: is functional morphology important? *Aquat. Ecol.* 50 (1), 45–57. <https://doi.org/10.1007/s10452-015-9551-2>.
- Perez-Escudero, A., de Polavieja, G., 2011. Collective animal behavior from Bayesian estimation and probability matching. *Nat. Proc.* <https://doi.org/10.1038/npre.2011.5939.2>.
- Plew, D.R., Nikora, V.I., Larned, S.T., Sykes, J.R.E., Cooper, G., 2007. Fish swimming speed variability at constant flow: *Galaxias maculatus*. *N. Z. J. Mar. Freshwater Res.* 41 (2), 185–195. <https://doi.org/10.1080/00288330709509907>.
- Puertas, J., Cea, L., Bermúdez, M., Pena, L., Rodríguez, Á., Rabuñal, J.R., Balairón, L., Lara, A., Aramburu, E., 2012. Computer application for the analysis and design of vertical slot fishways in accordance with the requirements of the target species. *Ecol. Eng.* 48, 51–60. <https://doi.org/10.1016/j.ecoleng.2011.05.009>.
- Rahel, F.J., McLaughlin, R.L., 2018. Selective fragmentation and the management of fish movement across anthropogenic barriers. *Ecol. Appl.* 28 (8), 2066–2081. [https://doi.org/10.1016/0584-8539\(78\)80068-3](https://doi.org/10.1016/0584-8539(78)80068-3).
- Reynolds, O., 1883. An experimental investigation of the circumstances which determine whether the motion of water shall be direct or sinuous, and of the law of resistance in parallel channels. *Philosop. Trans. R. Soc. Lond.* 174, 935–982.
- Sfakiotakis, M., Lane, D.M., Davies, J.B.C., 1999. Review of fish swimming modes for aquatic locomotion. *IEEE J. Ocean. Eng.* 24 (2), 237–252. <https://doi.org/10.1109/48.757275>.
- Tierney, K.B., Kasurak, A.V., Zielinski, B.S., Higgs, D.M., 2011. Swimming performance and invasion potential of the round goby. *Environ. Biol. Fishes* 92 (4), 491–502. <https://doi.org/10.1007/s10641-011-9867-2>.
- Tsikata, J.M., Tachie, M.F., Katopodis, C., 2014. Open-channel turbulent flow through bar racks. *J. Hydraul. Res.* 52 (5), 630–643. <https://doi.org/10.1080/00221686.2014.928805>.
- Tudorache, C., Viaene, P., Blust, R., Vereecken, H., De Boeck, G., 2008. A comparison of swimming capacity and energy use in seven European freshwater fish species. *Ecol. Freshw. Fish* 17 (2), 284–291. <https://doi.org/10.1111/j.1600-0633.2007.00280.x>.
- Wang, R.W., David, L., Larinier, M., 2010. Contribution of experimental fluid mechanics to the design of vertical slot fish passes. *Knowl. Manag. Aquat. Ecosyst.* 369 (02). <https://doi.org/10.1051/kmae/2010002>.
- Williams, J.G., Armstrong, G., Katopodis, C., Larinier, M., Travade, F., 2012. Thinking like a fish: a key ingredient for development of effective fish passage facilities at river obstructions. *River Res. Appl.* 28 (4), 407–417. <https://doi.org/10.1002/rra>.